7024 *Macromolecules* **2009**, *42*, 7024–7030
DOI: 10.1021/ma900816k

Macromolecules
ARTICLE

Probing the Natural-Abundance ^{13}C Populations of Insoluble Elastin Using $^{13}C-^{1}H$ Heteronuclear Correlation (HETCOR) NMR Spectroscopy

Kosuke Ohgo, Walter P. Niemczura, and Kristin K. Kumashiro*

Department of Chemistry, University of Hawaii, Honolulu, Hawaii 96822

Received April 14, 2009; Revised Manuscript Received August 3, 2009

ABSTRACT: The complexities of fibrous proteins in their native states often preclude the use of high-resolution solid-state NMR spectroscopy, particularly those utilizing multiple dimensions. In this study, the application of solid-state $^{13}C-^{1}H$ heteronuclear correlation spectroscopy with frequency-switched Lee−Goldburg decoupling (FSLG-HETCOR) to an unenriched sample of native elastin is reported. These 2D experiments on lyophilized and hydrated elastin illustrate that individual contributions to the overall profile in the aliphatic region of its ^{13}C spectrum may be resolved. As a result, details of side-chain packing in the hydrated and dehydrated elastin are elucidated. Generally, the HETCOR data show that the removal of water produces a compact state in this protein.

Introduction

Elastin is a complex biopolymer that is assembled from a high-molecular-weight monomer.[1] Eponymously named, elastin is the elastic component of vertebrate tissue types that must have both elasticity and resiliency for proper function. Skin and blood vessels are two prominent examples. Native elastin's extensive cross-linking and significant hydrophobic makeup[2] preclude solution NMR spectroscopy and X-ray diffraction, thereby adding to the challenge of elucidating this protein's structure−function relationships.

Although this lab and others have made progress in the detailed characterization of elastin and its mimetics using isotopic enrichment,[3−5] there is nevertheless great interest in using experiments that may be done with unenriched samples, particularly for a complex system such as this one. Sample preparation of elastin from abundant sources such as tissue is straightforward, and the concern about biological relevance, such as is often the criticism with simplified mimetic peptides, is minimized. However, the issues of spectral overlap which come with a system as complex as elastin make assignment and interpretation of 1D spectra difficult.

Two-dimensional NMR methods are classically grouped into three categories, that is, separation, exchange, and correlation. Application of these methods to complex systems, such as proteins like elastin, is always a challenge, as the issues of sample preparation and spectral overlap, among others, often render NMR to be somewhat limited in its usefulness.

The heteronuclear correlation (HETCOR) experiment is a deceptively simple concept, i.e., the correlation of nuclei of different magnetogyric ratios via the dipolar coupling. Initially, its widespread implementation was limited by the technical challenges posed by using homonuclear ^{1}H decoupling during the t_1 evolution period. Early applications of the HETCOR sequence utilized a CRAMPS scheme.[6,7] Recently, van Rossum and co-workers showed that a robust and easily implemented version of HETCOR[8] may be used with frequency-switched Lee−Goldburg (FSLG) decoupling,[9] rather than, e.g., BLEW-24[10] or other such decoupling schemes. FSLG-HETCOR has been applied to unenriched biopolymers such as chitins[11] or homopolypeptides[12] to obtain the chemical shift and/or spatial information. Hence, this FSLG-HETCOR experiment seems nearly ideal for our consideration of elastin.

In this study, we demonstrate that FSLG-HETCOR may be used to characterize elastin. This approach demonstrates the utility of FSLG-HETCOR for even large, complex systems without any isotopic enrichment. Moreover, it uncovers new information about the packing of residues in elastin that has not been reported previously, with any other technique. As expected, the directly bound $^{13}C-^{1}H$ spin pairs are observed with shortest mixing times, as are other intraresidue couplings. However, the great utility of this method for uncovering packing between the various residues (i.e., inter-residue and possibly interdomain) is demonstrated here. To calibrate our measurements, we preface the elastin studies with results for a crystalline sample of an amino acid salt.

Experimental Section

Elastin samples were purified from bovine nuchal ligament using the cyanogen bromide treatment, as described previously.[13] Typical sample sizes were 22 and 55 mg for the lyophilized and hydrated elastin samples, respectively. L-Tyrosine hydrochloride (Sigma-Aldrich, Saint Louis, MO) was used without further purification. L-Tyr·HCl is a crystalline salt. The sample size was 53 mg. Rotors were sealed from moisture with a top spacer fitted with fluorosilicone micro O-rings (Apple Rubber Products, Lancaster, NY).[14] O-ring seals are necessary to maintain the hydration level of hydrated elastin (60 mass % water) during data collection. Top and bottom spacers are machined from Kel-F for reduced ^{13}C background signal.

NMR data were acquired on a Varian Unity Inova WB 400 spectrometer, equipped with a 4 mm HXY-T3 MAS probe (Chemagnetics/Varian NMR, Fort Collins, CO). The spinning speed used in MAS experiments was 10 kHz. The pulse sequence for the 2D FSLG-HETCOR NMR experiments[8] is shown in Figure 1.

The proton rf field strength was set to 78.1 kHz during the t_1 delay for FSLG decoupling and during acquisition for TPPM decoupling.[15] For FSLG, $\tau = 10.4\ \mu s$ with the offset frequency

*Corresponding author: Tel (808) 956-5733, Fax (808) 956-5908, e-mail kumashir@hawaii.edu.

 Published on Web 08/21/2009

ΔLG of 55.2 kHz. The length of the magic-angle pulse with flip angle $\theta_m = 54.7°$ was 1.95 μs, corresponding to 3.2 μs for the ^{1}H 90° pulse. The efficiency of the FSLG decoupling was additionally optimized by offset-tuning of the probe observing a $^1J_{CH}$ splitting of [2-^{13}C]Gly (99%, Cambridge Isotope Laboratories, Andover, MA) obtained with CP/MAS and FSLG decoupling during acquisition. A linear ramped-amplitude (RAMP) CP sequence[16] was used to obtain a broader matching profile. The average field strength of CP was $(\gamma B_1/2\pi)$ = 53.4 kHz, with a linear ramp width of 9.5 kHz. The varied contact times were applied to obtain the spatial information based on the CP process. Recycle delays were 5 and 3 s for L-Tyr·HCl and elastin, respectively. The phase of the ^{1}H RAMP-CP spin-lock pulse was incremented as in a States method.[17] Data were acquired at 37 °C.

^{13}C chemical shifts were referenced to the tetramethylsilane scale, using hexamethylbenzene as an external standard [$\delta(^{13}CH_3)$ = 17.0 ppm at 37 °C]. ^{1}H chemical shifts were externally referenced by setting the Hβ resonance of the L-alanine at 1.0 ppm. The ^{1}H chemical shift scaling factor for FSLG experiments was determined from the slope of a plot of scaled L-alanine chemical shifts obtained from a FSLG experiment against the nonscaled proton chemical shifts from a ^{1}H fast MAS experiment. The average scaling factor was 0.53, which was slightly lower than the theoretical factor $\cos(\theta_m) = 1/\sqrt{3} = 0.577$.[18]

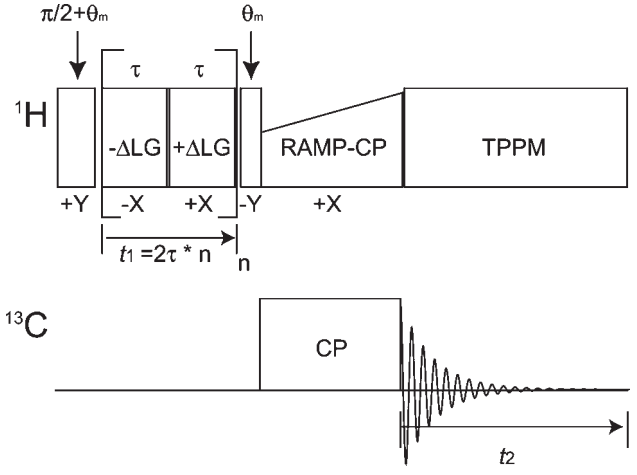

Figure 1. Pulse sequence for the 2D HETCOR NMR spectrum with FSLG decoupling.[8]

Results and Discussion

1. Calibration of Detection Ranges Using Tyrosine Hydrochloride. L-Tyrosine hydrochloride (L-Tyr·HCl, Figure 2) was chosen as the calibration standard for several reasons. The unenriched compound is cheaply and readily available from commercial sources in its crystalline form. Hence, straight from the bottle, it has well-resolved peaks in the ^{13}C CPMAS spectrum, allowing a relatively straightforward assignment of intra- and intermolecular ^{13}C−^{1}H spin pairs. Also note that the first report of the FSLG-HETCOR experiment used *U*-^{13}C L-Tyr·HCl to demonstrate the robustness of the approach, and full assignments were reported therein.[8]

Tables 1 and 2 list the intra- and intermolecular distances obtained from the published crystal structure.[19] The directly bound ^{13}C−^{1}H spin pairs (∼1.1 Å) are indicated in bold in Table 1. Briefly, there are two molecules per unit cell in the space group $P2_1$, a = 11.083 Å, b = 9.041 Å, c = 5.099 Å, and β = 91.82°. As a result of close packing, some of the ^{13}C−^{1}H distances between adjacent tyrosine salts are relatively short (< 3.0 Å).

Figures 3a, 3b, and 3c show the HETCOR spectra obtained for the microcrystalline L-Tyr·HCl sample with contact times of 50, 200, and 500 μs, respectively. The color contours indicate the relative peak intensity as strong (s, with relative intensity = 0.7−1.0), medium (m, 0.4−0.7), or weak (w, 0.1−0.4).

With the short 50 μs contact time (Figure 3a), strong intensities are observed only for directly bound ^{13}C−^{1}H spin pairs, such as with the ^{13}Cα and the unsubstituted ring carbons ^{13}Cδ1, ^{13}Cδ2, ^{13}Cε1, and ^{13}Cε2. The high intensities are consistent with the short (∼1.1 Å) distances. Medium-intensity cross-peaks are seen between a given ^{1}H nucleus and the ^{13}C that is two bonds away, such as with ^{13}Cβ−^{1}Hα, as well as the analogous correlations involving the unsubstituted ring carbons. Weak correlations from ^{13}Cα and ^{13}Cβ to ring protons, most likely ^{1}Hδ2, are also observed. Very

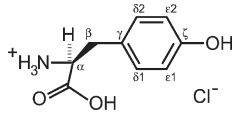

Figure 2. Chemical structure of L-tyrosine·HCl.

Table 1. Intramolecular ^{13}C−^{1}H Distances (Å) Obtained from Crystalline Structure

	COOH, 172 ppm	Cζ, 152 ppm	Cδ1, 133 ppm	Cδ2, 129 ppm	Cγ, 126 ppm	Cε2, 118 ppm	Cε1, 115 ppm	Cα, 57 ppm	Cβ, 37 ppm
$H_2\beta$	2.7, 3.4	4.8, 4.8	2.6, 3.3	2.8, 3.4	2.1, 2.2	4.1, 4.6	4.0, 4.5	2.1, 2.1	**1.1**
Hα	2.2	5.1	4.0	3.0	2.8	4.2	5.0	**1.1**	2.2
Hε2	5.6	2.2	3.9	2.2	3.4	**1.1**	3.4	5.2	4.7
Hδ1	3.6	3.4	**1.1**	3.4	2.1	3.9	2.1	3.8	2.7
Hε1	5.4	2.2	2.2	3.9	3.4	3.4	**1.1**	5.7	4.7
Hδ2	4.0	3.4	3.4	**1.1**	2.2	2.2	3.9	3.1	2.7
HO	6.8	2.0	3.9	4.4	4.7	3.2	2.5	7.0	6.2
HOOC	1.9	5.0	4.0	4.3	3.8	4.9	4.6	3.2	4.0
H_3N	2.6. 2.7, 3.3	6.8. 6.9, 7.2	5.0, 5.1, 5.6	4.6, 5.1, 5.1	4.0, 4.2. 4.6	6.0, 6.4, 6.5	6.3, 6.4, 6.8	2.1, 2.1, 2.1	2.6. 2.8. 3.4

Table 2. Intermolecular ^{13}C−^{1}H Distances (Å) (Listed up to 4 Å) Obtained from Crystalline Structure

COOH		Cζ		Cδ1		Cδ2		Cγ		Cε2		Cε1		Cα		Cβ	
HN	3.0	HOOC	2.5	Hε2	2.9	Hδ1	2.9	Hε1	3.2	Hδ1	2.7	Hε2	2.8	Hβ	3.6	Hε1	3.1
Hβ	3.5	Hδ1	3.3	Hε2	3.1	Hε1	3.0	Hε2	3.3	HOOC	2.9	Hβ	3.3	HN	3.8	Hδ2	3.3
HN3	3.5	Hε2	3.3	Hδ2	3.7	Hβ	3.1	Hδ1	3.6	Hδ1	3.1	Hδ2	3.4			Hε2	3.6
HN	3.6	Hδ1	3.3	Hε2	3.9	Hβ	3.4	Hε2	3.6	Hβ	3.4	Hδ2	3.6			Hα	3.6
Hε2	3.8	Hδ2	3.4			Hδ1	3.7	Hβ	3.7	Hβ	3.7	Hε2	3.6				
HO	3.9	Hε1	4.0			HO	3.7	Hδ2	4.0	Hε1	3.7	HOOC	3.7				
						Hε2	3.9			Hε1	3.9	Hδ1	3.9				
						Hε1	3.9			Hε2	3.9	Hδ1	3.9				

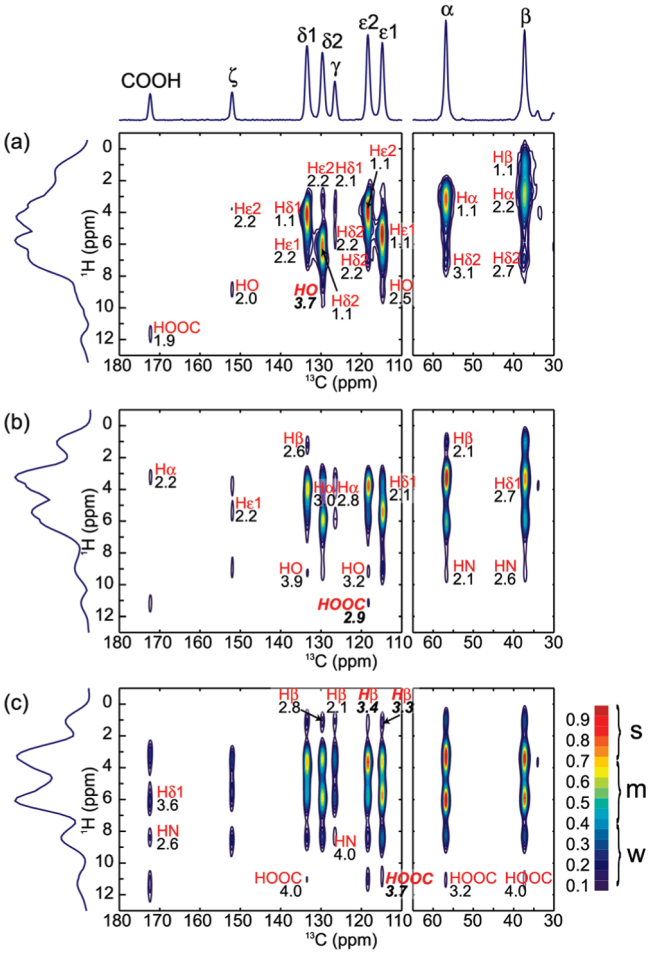

Figure 3. ^{13}C−^{1}H FSLG-HETCOR spectra of L-Tyr·HCl with contact times of (a) 50 μs, (b) 200 μs, and (c) 500 μs. For each spectrum, the skyline projection along the ^{1}H dimension is shown. The ^{1}H assignments are shown together with the ^{13}C−^{1}H distance obtained from the crystalline structure. The assignments in bold italics indicate the intermolecular correlations.

weak cross-peaks for the phenolic proton and the unsubstituted ring carbons ^{13}Cδ2 and ^{13}Cε1 are also observed. If the medium- and high-intensity cross-peaks are used as a cutoff, then the reliably detectable range of distances for this short CP time of 50 μs is ~2.2 Å and less. The decision to use the stronger intensities as the central criterion is particularly relevant for our application to magnetically dilute systems such as unenriched elastin samples.

It is noted that ^{1}H chemical shifts of Hδ1 and Hε2 are shifted upfield by ~1.5−2 ppm from those of Hδ2 and Hε1. The upfield shift of the ring protons in the solid state was reported previously.[20]

When the contact time is increased to 200 μs, the spectrum of Figure 3b is observed. More couplings in the 1.9−2.2 Å range are observed, in addition to medium-to-weak couplings 3 Å apart, typically involving one of the protons on the ring. Very weak correlations of ^{13}Cδ2−OH and ^{13}Cδ1−OH correspond to long distances with 3.7 and 3.9 Å, respectively. Again, the criterion for the upper limit of detection via FSLG-HETCOR is intensity (medium or high). Hence, the upper limit of detectable correlations for the 200 μs contact time is 3 Å.

Finally, with the 500 μs contact time, the detectable range is increased to an upper limit of ~4 Å. Higher cross-peak intensities are observed for the shorter distances, as compared to the 50 or 200 μs data. For example, the downfield carboxylate ^{13}C has stronger cross-peaks with the Hα and the carboxylate ^{1}H than seen in the 200 μs spectrum. In addition, however, there are correlations to the ^{1}HN and to the proton(s) on the ring. Furthermore, intermolecular correlations between ^{13}Cε1−Hβ (3.3 Å), ^{13}Cε2−Hβ (3.4 Å), and ^{13}Cε1−HOOC (3.7 Å) can be seen in the spectrum.

Table 3. Summary of the FSLG-HETCOR Experiments for L-Tyr·HCl[a]

contact time (μs)	^{13}C−^{1}H correlation	distance (Å)
50	m−s:direct bonded C−H	1.1
	m:Cβ−Hα	2.2
	w:Cβ−Hδ2	2.7
	w:Cα−Hδ2	3.1
	w:Cε1−HO	2.5
	w:Cε2−Hδ2	2.2
	w:Cδ2−Hε2, ***HO***	2.2, ***3.7***
	w:Cδ1−Hε1	2.2
	w:Cγ−Hδ1, Hδ2	2.1, 2.2
	w:Cζ−HO, Hε2	2.0, 2.2
	w:C=O−HOOC	1.9
200	m:Cβ−Hδ1	2.7
	w:Cβ−HN	2.6
	w:Cα−Hβ, HN	2.1
	w:Cε1−Hδ1	2.1
	w:Cε2−***HOOC***, HO	***2.9***, 3.2
	w:Cγ−Hα	2.8
	w:Cδ2−Hα	3.0
	w:Cδ1−Hβ, HO	2.6, 3.9
	w:Cζ−Hε1	2.2
	w:C=O−Hα	2.2
500	w:Cβ−HOOC	4.0
	w:Cα−HOOC	3.2
	w:Cε1−***Hβ***, ***HOOC***	***3.3***, ***3.7***
	w:Cε2−***Hβ***	***3.4***
	w:Cγ−Hβ, HN	2.1, 4.0
	w:Cδ2−Hβ	2.8
	w:Cδ1−HOOC	4.0
	w:C=O−HN, Hδ1	2.6, 3.6

[a] s = strong (0.7−1.0), m = medium (0.4-0.7), w = weak (0.1−0.4). Bold italics: intermolecular correlation.

The results of the HETCOR experiments on the Tyr·HCl are summarized in Table 3. They demonstrate that, roughly speaking, the heteronuclear spin pairs within 2.2, 3, and 4 Å are selected with contact times of 50, 200, and 500 μs. (In practice, however, the shortest CP time also incurs a severe limit on the amount of signal that may be detected.) These data are also consistent with the findings of Baldus and coworkers,[21] who presented a theoretical picture for the C−H−H−C transfer via cross-polarization and spin-diffusion for the ^{13}C−^{1}H and ^{1}H−^{1}H spin pairs, respectively. Buildup curves for the L-Tyr·HCl (see the Supporting Information) are comparable to those of His·HCl in the previous study, namely, that the distance dependence of polarization transfer is roughly preserved, even in this simpler scheme.

2. Characterization of ^{13}C−^{1}H Correlations in Lyophilized Elastin. Evidence for a Compact Structure. The HETCOR spectra of lyophilized elastin are illustrated in Figure 4. Only the aliphatic region is shown, for simplicity. Horizontal and vertical guidelines are used with tentative assignments of the ^{1}H and ^{13}C, respectively. These assignments are based on previous studies of elastin[13,22−24] and aggregate data in the Biological Magnetic Resonance Data Bank.[25]

Briefly, glycine (Gly), proline (Pro), alanine (Ala), and valine (Val) account for over 80% of the amino acids in elastin.[2] Elastin is most often described as having hydrophobic and cross-linking domain types, largely in an alternating cassette organization. Gly, Pro, and Val are found in the hydrophobic domain type, whereas Ala is a component in both.

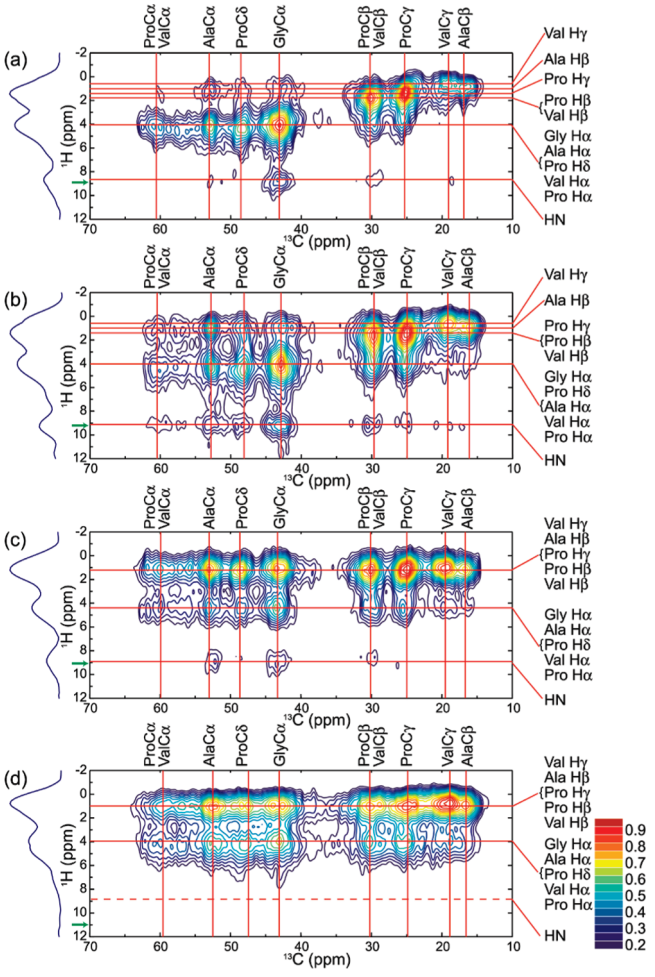

Figure 4. ^{13}C−^{1}H FSLG-HETCOR spectra of lyophilized elastin with contact times of (a) 200 μs, (b) 500 μs, and (c) 1500 μs. The spectrum of the NH/ND exchanged sample with contact time of 1500 μs is shown in (d). For each spectrum, the skyline projection along the ^{1}H dimension is shown. Green arrows indicate the center of the ^{1}H spectral window.

The 200 μs contact time is used to select for short-range (≤3 Å) interactions, based on the results on the Tyr·HCl calibration standard. As illustrated in Figure 4a, the strongest cross-peaks are observed for the ^{13}Cα-Gly and ^{13}Cγ-Pro as well as the feature that includes both ^{13}Cβ-Pro and ^{13}Cβ-Val. Presumably, these high intensities are due to the fact that most of these directly bound spin pairs are methylene (−CH_2−) groups, effecting high relative cross-polarization efficiencies with two directly bound protons for each carbon. Weaker correlations are seen with the methyl groups at 16 and 19 ppm, assigned to ^{13}Cβ-Ala and ^{13}Cγ-Val, as well as some of the ^{13}Cα carbons of, especially, Ala, Val, and Pro. Very weak correlations for spin pairs separated by ∼2.2 Å are also observed, including those to the amide proton as well as correlations from the ^{13}Cα to protons further down the side chain.

Perhaps one of the most surprising results of the spectrum acquired with the 200 μs contact time data is the weak cross-peak that arises between ^{13}Cα-Gly and the upfield region of the ^{1}H chemical shift scale, typically assigned to methyl groups, such as found in Val and Ala. This upfield region in the ^{1}H chemical shift range is also assigned to protons in the Pro ring. As there are no upfield ^{1}H sites in glycine, methyl or otherwise, it is apparent that this experiment provides evidence for tight hydrophobic packing in the Gly-rich hydrophobic domains. It is noted that the ^{13}Cα-Gly peak is well-resolved;[26] i.e., very seldom is another residue's carbon observed with this chemical shift.

Another noteworthy feature of this HETCOR spectrum is the resolution of overlapping peaks in the ^{1}H dimension, especially. For instance, the ^{1}Hγ-Pro peak has a chemical shift that is slightly upfield from the ^{1}Hβ-Pro and ^{1}Hβ-Val features, whereas it is downfield-shifted from the methyls of Val and Ala. These differences are not as apparent at higher contact times, when the excitation across the entire sample becomes increasingly more uniform, and subtle differences in dynamics are not as easily distinguishable.

When the contact time is increased to 500 μs, the spectrum of Figure 4b is observed. The peaks noted in the 200 μs spectrum are stronger. The correlations from ^{13}Cα-Gly and ^{13}Cγ-Pro to the neighboring ^{1}H, as well as the overlapping peaks of ^{13}Cβ-Pro and ^{13}Cβ-Val, are higher in intensity. Three cross-peaks from ^{13}Cα-Ala to various protons, including the ^{1}HN-Ala, ^{1}Hα-Ala, and ^{1}Hβ-Ala, are observed. In fact, most of the Cα carbons show at least three resonances, although the ones corresponding to the upfield region are strong, likely due to high CP efficiencies at short times for these −CH− and −CH_2− carbons, as well as relative abundance in the protein. The latter point is especially true for the glycines, which comprise over 1/3 of the protein's residues.[2] Correlations from the upfield aliphatic carbons (< 35 ppm) are also seen, as expected, reflecting weak interactions between, for example, the Cβ carbons to the ^{1}H of the backbone amides. In addition, the cross-peaks from ^{13}Cγ and ^{13}Cδ of Pro to ^{1}HN indicate inter-residue correlations between Pro and the other residues; as with the analogous case of the GlyCα correlations at the short contact time, there is no amide proton in proline residues. Hence, these cross-peaks must reflect inter-residue (not intraresidue) proximity.

At 500 μs, correlations are observed between Gly Cα and the upfield region, most likely methyl protons of Ala or Val residues. In fact, the dipeptide units of Gly-Val, Gly-Ala, and Val-Gly appear frequently in the primary sequence of tropoelastin.[2] A search of the Research Collaboratory for Structural Bioinformatics Protein Data Bank[27] (http://www.pdb.org/) for proteins with Gly-Val, Val-Gly, or Gly-Ala sequences provides more evidence that this correlation may be due to close proximity of these amino acids. Crystallographic data give minimum distances between Gly Cα and Val Hγ to be 3.6 Å in GV and VG. Analogously, the closest approach between Gly Cα and Ala Hβ is 3.2 Å in GA.

Finally, a HETCOR spectrum is recorded with a 1.5 ms contact time. The strongest signals are due to the upfield ^{1}H at ∼1.2 ppm to the resolved carbons. Weak-to-medium correlations to the Hα are also observed, in addition to a few to the ^{1}HN. At this point, it is reasonable to assume that signals in a typical solid are either near maximum or are already decreased due to $T_{1\rho}$ decay.

As an additional check, the elastin was swollen for 56 h in D_2O and then lyophilized. Figure 4d illustrates the HETCOR spectrum that is obtained with the H/D exchanged sample. Here, there are no more cross-peaks in the amide region. The rest of the spectrum looks nearly identical to the unexchanged spectrum, confirming earlier work that the entire protein is undergoing rapid fluctuations in the hydrated state and that all backbone amide protons are solvent-accessible.[4,13,23,28]

3. Characterization of ^{13}C−^{1}H Correlations in Hydrated Elastin. The HETCOR spectrum acquired with the 200 μs contact time is illustrated in Figure 5a. As expected, the spin pairs separated by 3 Å or less are detected. These assignments include the directly bound ^{13}Cα and ^{1}HN, although weak, as

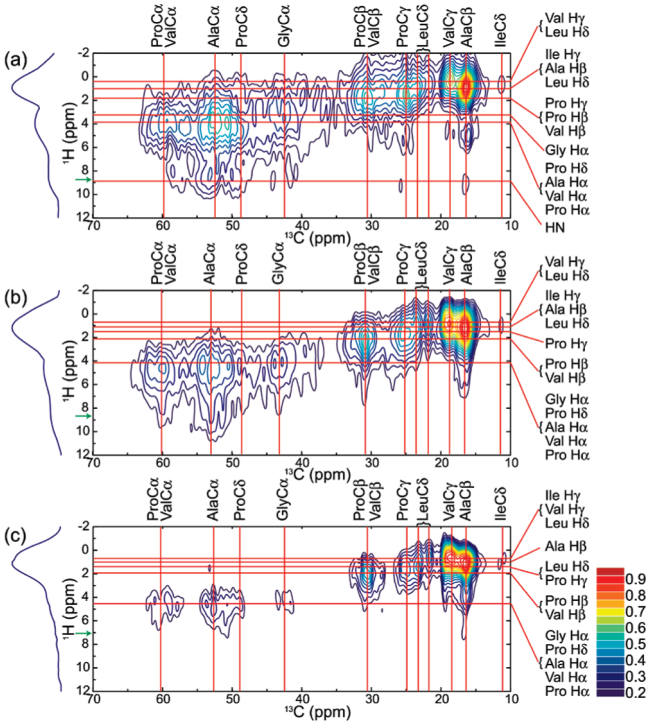

Figure 5. ^{13}C−^{1}H FSLG-HETCOR spectra of hydrated elastin with contact time of (a) 200 μs, (b) 500 μs, and (c) 1000 μs. For each spectrum, the skyline projection along the ^{1}H dimension is shown. Green arrows indicate the center of the ^{1}H spectral window.

well as the correlations originating from, particularly, the methyl groups.

The strongest cross-peak in the spectrum is the one corresponding to the upfield methyl group ((^{13}C)δ = 16.4 ppm). Interestingly, it is resolved from the other methyl group ((^{13}C)δ = 18.6 ppm) in both ^{13}C and ^{1}H dimensions. Also, a weak correlation between ^{13}Cα-Ala ((^{13}C)δ = 52.5 ppm) and ^{1}Hβ-Ala is observed. The chemical shifts of the peaks assigned to Ala are consistent with reports describing this residue in α-helices.[29−31]

As the contact times are increased to 500 μs (Figure 5b) and 1 ms (Figure 5c), the spectra simplify. The correlations to the amide protons are lower in intensity in Figure 5b and then disappear with the longest CP time. This result is consistent with previously reported work by this group[13] and others,[23] which noted the low CP intensities and corresponding fast motions that contribute to short $T_{1\rho}$ values.

The intensities of the methyl cross-peaks, however, increase with contact time, unlike the rest of the spectrum. Furthermore, the ratio of upfield-to-downfield methyl peaks differs from that of the lyophilized sample. In the latter, the upfield methyl peak has lower intensity than the downfield, but the opposite is true in the hydrated sample. In the primary sequence of bovine tropoelastin, there are 155 Ala and 92 Val residues,[2] and thus, the corresponding numbers of methyl carbons are counted as 155 (Ala) and 184 (Val). If the mobilities of two types of carbons are comparable, then their intensities in a CP spectrum reflect the relative populations. The lyophilized sample has such an quantitative line shape. On the other hand, the intensity of ^{13}Cβ-Ala ((^{13}C)δ = 16.4 ppm) is stronger than that of ^{13}Cγ-Val ((^{13}C)δ = 18.6 ppm) in the hydrated sample. This result provides strong evidence for Ala-rich segments to be located in regions of lower mobility than found elsewhere in the sample; i.e., the α-helical Ala methyls have better CP efficiency than the Val. As noted above, most of the Val is found in the hydrophobic

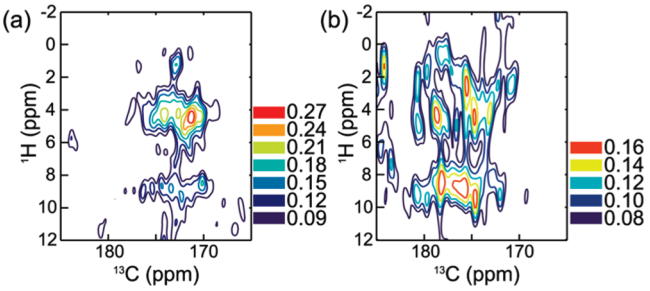

Figure 6. Downfield region of the HETCOR spectra of lyophilized (a) and hydrated (b) elastin, taken with the 200 μs contact time. ^{13}C chemical shifts correspond to the backbone $^{13}C_{C=O}$ nuclei. The entire ^{1}H chemical shift region is shown in both spectra. The contour plots are referenced to the same scale as the aliphatic regions of Figures 4 and 5, whereby the tallest peak in the entire spectrum is set to 1.0.

domain types, whereas the α-helical Ala is found in the cross-linking regions.

It is also noted that ^{13}C peaks at 21.8 and 23.3 ppm are clearly visible in the HETCOR spectra of hydrated elastin, particularly with the longer contact times. These peaks were also distinguishable in a 1D ^{13}C CPMAS spectrum of hydrated elastin,[13] although tentative assignments then were not made. The resolution in the spectra of lyophilized elastin[13] and elastin peptides[3] is considerably less, so the peaks at 21.8 and 23.3 ppm are not clearly resolved in dehydrated elastin samples.

HETCOR data of the hydrated sample show that these peaks at 21.8 and 23.3 ppm have correlations to the methyl and methylene protons, based on the ^{1}H chemical shift of the cross-peaks. One of the possible assignments for those peaks is Leu Cδ1 and Cδ2 methyl carbons, which have typical ^{13}C chemical shifts in the range of ∼20−24 ppm, according to the RefDB chemical shift database.[26] The number of Leu residues in the bovine elastin is 50, which is the third-most abundant residue with methyl carbons (after Ala and Val). Similar peaks were observed in the hydrated elastin.[23]

The HETCOR spectra in the region of the backbone carbonyl carbons are shown in Figure 6. The contact time used for these experiments of Figure 6 is 200 μs. In the lyophilized sample, the peak intensities are weak, as expected.

The intensities of these cross-peaks are only about a fourth of the tallest feature in the entire spectrum, i.e., in the aliphatic region. The backbone carbonyls are nonprotonated, so it is expected that, in a typical solid, the maximum peak intensities are seen with longer CP times, e.g., 1 ms. The most intense cross-peak has a peak position of 172 ppm, which is consistent with the 1D ^{13}C CPMAS NMR spectrum of lyophilized elastin, reported previously.[13]

In the presence of water, however, a surprising amount of information is seen in this region of the spectrum (Figure 6b). Specifically, although the intensity of any given peak in the HETCOR data of the hydrated sample is lower than that observed at the highest point of the other spectrum, there are many more resolved features than seen for the lyophilized elastin. Furthermore, there are many cross-peaks in the downfield regions of the spectrum, corresponding to α-helical carbons.[29−31] This latter result is consistent with what is happening in the upfield region, such as with the prominent methyl feature.

As noted above, elastin is typically described in the context of its two domain types, hydrophobic and cross-linking. The former consists mostly of Gly, Val, and Pro, with smaller amounts of Ala, Leu, and Ile.[2] Many of the cross-linking domains are described as polyalanine regions with lysines

and heteroaromatic desmosine cross-links in tropoelastin and insoluble elastin, respectively. With its high Ala content, it is not surprising that measurements of soluble elastin peptides reflect the correspondingly high α-helical content.[32] In addition, however, the HETCOR data of the hydrated sample provide strong spectroscopic evidence that the secondary structural motifs are preserved, even in the limits of fast motion manifest in narrow lines and poor CP efficiencies. Furthermore, the motion is slower than that of the hydrophobic domains, even if only by a small amount. Again, this result is consistent with previous work,[13] but the application of HETCOR brings information about specific residue types to light.

Conclusion

The traditional approaches for structural studies of large proteins using solid-state NMR spectroscopy have typically focused on circumventing the inherent complexities of these systems. Namely, examining a mimetic brings fewer ambiguities of data interpretation. However, the mimetics only provide a portion of the overall picture, as they typically focus on, e.g., only the hydrophobic domains. For many ssNMR studies, it is possible to do isotopic enrichment via bacterial expression of the native sequence. This approach is now standard for membrane proteins over a large range of molecular weights.[33] However, elastin has only recently been synthesized via this route,[34] no doubt due to the high molecular weight of the soluble monomer as well as the challenges of fabricating a cross-linked material that closely mimics the native system. Here we note that we recently reported a solid-state NMR study of a 5-domain mimetic of elastin,[22] but it only described the un-cross-linked peptide. Native elastin can be purified in large quantities from tissue. Hence, while the strategies of isotopically enriched elastin mimetics for solid-state NMR spectroscopy are refined, new approaches for the characterization of unenriched samples are pursued.

This study shows conclusively that useful HETCOR spectra may be obtained from unenriched protein at only moderate field strengths and sample spinning speeds. Peaks in regions of severe overlap are resolved in the indirect dimension, and assignment becomes significantly less ambiguous than when limited to a single dimension.

Furthermore, for this particular protein, this approach is extremely useful in numerous ways. First, these results are completely consistent with previously published work on elastin[4,13] as well as an elastin mimetic.[35] For instance, the low CP efficiencies of the hydrated elastin due to the fast motions throughout the protein are noted. In addition, however, the HETCOR provides the spectroscopic evidence for a compact state when water is removed.[36] Specifically, the resolved ^{13}Cα-Gly has a cross-peak with the methyl region with short contact time. This 200 μs CP time, in effect, serves as a "filter" for internuclear distances of 3 Å or less. This collapse of the hydrophobic region was proposed in earlier studies, including the proteolytic study that first described the "oiled coil" model of elastin.[37]

Even more information about elastin is revealed in the analysis of the hydrated sample. Here, the CP efficiencies are indicative of a mobile system. However, this data indicates that the Ala-rich regions, presumably the cross-linking domains, undergo motions that may be slower than the hydrophobic ones. Furthermore, the isotropic chemical shifts, namely, the appearance of downfield backbone carbonyls and upfield methyls,indicate that the Ala-rich segments have retained their α-helical structures, even if undergoing rapid reorientation. Such a paradox had been reported earlier, in the 1D MAS studies of elastin with isotopic enrichment of the glycine populations.[4] The FSLG-HETCOR experiment can clearly be a useful tool in the characterization of extensive biopolymers, such as elastin. Again, while the methodology for the preparation of isotopically enriched samples of complicated biomolecules is developed, the application to unlabeled materials is clearly a useful, easily implemented, and reasonably robust one.

Acknowledgment. This work was partially supported by a grant to K.K.K. from the National Science Foundation (MCB-0344975).

Supporting Information Available: Figures showing HETCOR buildup curves for each of the resolved carbons in unenriched L-Tyr·HCl (Figure S1) and comparison between the buildup curves and spin-diffusion curves from ref 21 (Figure S2). This material is available free of charge via the Internet at http://pubs.acs.org.

References and Notes

(1) Rosenbloom, J.; Abrams, W. R.; Mecham, R. *FASEB J.* **1993**, *7*, 1208–1218.
(2) Raju, K.; Anwar, R. A. *J. Biol. Chem.* **1987**, *262*, 5755–5762.
(3) Kumashiro, K. K.; Ohgo, K.; Niemczura, W. P.; Onizuka, A. K.; Asakura, T. *Biopolymers* **2008**, *89*, 668–679.
(4) Perry, A.; Stypa, M. P.; Foster, J. A.; Kumashiro, K. K. *J. Am. Chem. Soc.* **2002**, *124*, 6832–6833.
(5) Yao, X. L.; Hong, M. *J. Am. Chem. Soc.* **2004**, *126*, 4199–4210.
(6) Caravatti, P.; Bodenhausen, G.; Ernst, R. R. *Chem. Phys. Lett.* **1982**, *89*, 363–367.
(7) Roberts, J. E.; Vega, S.; Griffin, R. G. *J. Am. Chem. Soc.* **1984**, *106*, 2506–2512.
(8) vanRossum, B. J.; Forster, H.; deGroot, H. J. M. *J. Magn. Reson.* **1997**, *124*, 516–519.
(9) Bielecki, A.; Kolbert, A. C.; Levitt, M. H. *Chem. Phys. Lett.* **1989**, *155*, 341–346.
(10) Gu, Z. T.; Ridenour, C. F.; Bronnimann, C. E.; Iwashita, T.; McDermott, A. *J. Am. Chem. Soc.* **1996**, *118*, 822–829.
(11) Kono, H. *Biopolymers* **2004**, *75*, 255–263.
(12) Murata, K.; Kono, H.; Katoh, E.; Kuroki, S.; Ando, I. *Polymer* **2003**, *44*, 4021–4027.
(13) Perry, A.; Stypa, M. P.; Tenn, B. K.; Kumashiro, K. K. *Biophys. J.* **2002**, *82*, 1086–1095.
(14) Martin, R. W.; Paulson, E. K.; Zilm, K. W. *Rev. Sci. Instrum.* **2003**, *74*, 3045–3061.
(15) Bennett, A. E.; Rienstra, C. M.; Auger, M.; Lakshmi, K. V.; Griffin, R. G. *J. Chem. Phys.* **1995**, *103*, 6951–6958.
(16) Metz, G.; Wu, X. L.; Smith, S. O. *J. Magn. Reson., Ser. A* **1994**, *110*, 219–227.
(17) States, D. J.; Haberkorn, R. A.; Ruben, D. J. *J. Magn. Reson.* **1982**, *48*, 286–292.
(18) Lee, M.; Goldburg, W. I. *Phys. Rev.* **1965**, *140*, A1261–1271.
(19) Frey, M. N.; Koetzle, T. F.; Koetzle, F.; Lehmann, M. S.; Hamilton, W. C. *J. Chem. Phys.* **1973**, *58*, 2547–2556.
(20) Saalwachter, K.; Graf, R.; Spiess, H. W. *J. Magn. Reson.* **1999**, *140*, 471–476.
(21) Lange, A.; Seidel, K.; Verdier, L.; Luca, S.; Baldus, M. *J. Am. Chem. Soc.* **2003**, *125*, 12640–12648.
(22) Kumashiro, K. K.; Ho, J. P.; Niemczura, W. P.; Keeley, F. W. *J. Biol. Chem.* **2006**, *281*, 23757–23765.
(23) Pometun, M. S.; Chekmenev, E. Y.; Wittebort, R. J. *J. Biol. Chem.* **2004**, *279*, 7982–7987.
(24) Kricheldorf, H. R.; Muller, D. *Int. J. Biol. Macromol.* **1984**, *6*, 145–151.
(25) Ulrich, E. L.; Akutsu, H.; Doreleijers, J. F.; Harano, Y.; Ioannidis, Y. E.; Lin, J.; Livny, M.; Mading, S.; Maziuk, D.; Miller, Z.; Nakatani, E.; Schulte, C. F.; Tolmie, D. E.; Wenger, R. K.; Yao, H. Y.; Markley, J. L. *Nucleic Acids Res.* **2008**, *36*, D402–408.
(26) Zhang, H. Y.; Neal, S.; Wishart, D. S. *J. Biomol. NMR* **2003**, *25*, 173–195.
(27) Berman, H. M.; Westbrook, J.; Feng, Z.; Gilliland, G.; Bhat, T. N.; Weissig, H.; Shindyalov, I. N.; Bourne, P. E. *Nucleic Acids Res.* **2000**, *28*, 235–242.
(28) Torchia, D. A.; Piez, K. A. *J. Mol. Biol.* **1973**, *76*, 419–424.
(29) Saito, H.; Tabeta, R.; Shoji, A.; Ozaki, T.; Ando, I. *Macromolecules* **1983**, *16*, 1050–1057.

(30) Kricheldorf, H. R.; Muller, D. *Macromolecules* **1983**, *16*, 615–623.
(31) Nakazawa, Y.; Asakura, T. *J. Am. Chem. Soc.* **2003**, *125*, 7230–7237.
(32) Miao, M.; Cirulis, J. T.; Lee, S.; Keeley, F. W. *Biochemistry* **2005**, *44*, 14367–14375.
(33) Lian, L. Y.; Middleton, D. A. *Prog. Nucl. Magn. Reson. Spectrosc.* **2001**, *39*, 171–190.
(34) Martin, S. L.; Vrhovski, B.; Weiss, A. S. *Gene* **1995**, *154*, 159–166.
(35) Yao, X. L.; Conticello, V. P.; Hong, M. *Magn. Reson. Chem.* **2004**, *42*, 267–275.
(36) Gosline, J. M. *Int. Rev. Connect. Tissue Res.* **1976**, *7*, 211−249 and references therein.
(37) Gray, W. R.; Sandberg, L. B.; Foster, J. A. *Nature* **1973**, *246*, 461–466.